HHS Public Access

Author manuscript

Hepatology. Author manuscript; available in PMC 2018 March 01.

Published in final edited form as:

Hepatology. 2017 March ; 65(3): 983–998. doi:10.1002/hep.28921.

The UPR mediates fibrogenesis and collagen I secretion through regulating TANGO1

Jessica L Maiers, **Enis Kostallari**, **Malek Mushref**, **Thiago M de Assuncao**, **Haiyang Li**, **Robert C Huebert**, **Sheng Cao**, **Harmeet Malhi**, and **Vijay H Shah**

Division of Gastroenterology and Hepatology, Mayo Clinic, Rochester, MN 55905

Abstract

Background/Aims—Fibrogenesis encompasses the deposition of matrix proteins such as collagen I by hepatic stellate cells (HSCs) that culminates in cirrhosis. Fibrogenic signals drive transcription of procollagen I, which enters the endoplasmic reticulum (ER), is trafficked through the secretory pathway, and released to generate extracellular matrix. Alternatively, disruption of procollagen I ER export could activate the unfolded protein response (UPR) and drive HSC apoptosis. Using a siRNA screen, we identified TANGO1 as a potential player in collagen I secretion. We investigated the role of TANGO1 in procollagen I secretion in HSCs and liver fibrogenesis.

Methods/Results—Depletion of TANGO1 in HSCs blocked collagen I secretion without affecting other matrix proteins. Disruption of secretion led to procollagen I retention within the ER, induction of the UPR, and HSC apoptosis. In wild-type HSCs, both TANGO1 and the UPR were induced by TGFβ. As the UPR upregulates proteins involved in secretion, we studied whether TANGO1 was a target of the UPR. We found that UPR signaling is responsible for upregulating TANGO1 in response to TGFβ, and this mechanism is mediated by the transcription factor XBP1. *In vivo*, murine and human cirrhotic tissue displayed increased TANGO1 mRNA levels. Finally, TANGO1$^{+/-}$ mice displayed less hepatic fibrosis compared to wild-type mice in two separate murine models: CCl_4 and BDL.

Conclusion—Loss of TANGO1 leads to procollagen I retention in the ER which promotes UPR-mediated HSC apoptosis. TANGO1 regulation during HSC activation occurs through a UPR dependent mechanism that requires the transcription factor XBP-1. Finally, TANGO1 is critical for fibrogenesis through mediating HSC homeostasis. Our work reveals a unique role for TANGO1 and the UPR in facilitating collagen I secretion and fibrogenesis.

Keywords

Hepatic Stellate Cell; fibrosis; Endoplasmic Reticulum apoptosis; XBP1

Introduction

Liver cirrhosis is the leading cause of end-stage liver disease and affects millions worldwide (1, 2). Cirrhosis is characterized by fibrogenesis, the secretion and deposition of

Address for correspondence: Vijay H. Shah, MD, Mayo Clinic, 200 First Street, SW, Rochester, MN 55905, shah.vijay@mayo.edu.

extracellular matrix proteins, which is primarily mediated by activated HSCs (1–4). The dominant matrix protein produced and secreted by HSCs is collagen I. Collagen I consists of two procollagen isoforms, α_1 and α_2 (139 and 129kD respectively), which are cotranslationally translocated into the ER. Once in the ER, procollagen I is folded with the help of several chaperones including BiP, protein disulfide isomerase (PDI), and the collagen-specific chaperone HSP47 (5–7). While the mechanisms of procollagen I folding are well established, procollagen I export from the ER is poorly understood (8). Furthermore, since procollagen I expression is increased in HSCs by fibrogenic signals, the proteins involved in ER export of procollagen I must be properly regulated to accommodate the increase in procollagen I trafficking and avoid disrupting cellular homeostasis.

An emerging protein that may regulate procollagen I export from the ER is TANGO1 (Transport And Golgi Organization 1) (9–11). TANGO1 was originally identified in a screen for proteins involved in Golgi organization (9). *In vitro* studies in chondrocytes found that TANGO1 specifically mediates procollagen VII export without affecting general protein secretion (10). Additionally, *in vivo* studies in TANGO1$^{-/-}$ mice found that global loss of TANGO1 is embryonic lethal due to skeletal abnormalities (11). While TANGO1 is clearly critical for early development, the importance of TANGO1 in collagen-mediated pathologies such as hepatic fibrogenesis remains unexplored.

Regulation of protein export from the ER is key to cellular homeostasis, as disruption of this process can lead to ER stress, and activation of the unfolded protein response (UPR). The UPR consists of 3 signaling pathways mediated by the ER membrane proteins inositol–requiring enzyme-1 alpha (IRE1α), activating transcription factor 6 alpha (ATF6α), and protein kinase RNA-like ER kinase (PERK). UPR signaling aims to reduce the ER protein load by repressing global protein translation and promoting expression of selective genes involved in protein folding, secretion, and degradation (12–14). Transcription factors such as X-box Binding Protein 1 (XBP1) and activating transcription factor 4 (ATF4) are critical for selective upregulation of UPR targets that facilitate resolution of ER stress (15). If TANGO1 is involved in procollagen I secretion, it is reasonable to predict that the UPR may regulate TANGO1 in response to increased procollagen I production during HSC activation, similar to beta cells in response to increased insulin secretion (16–18). If ER stress is unresolved, cells undergo apoptosis. Pro-apoptotic UPR signaling is mediated by the transcription factor CHOP and its target death receptor 5 (DR5, also known as TRAIL-R2) (19). As HSC apoptosis is favorable for fibrosis resolution, procollagen I retention in the ER and ensuing UPR signaling could have additional anti-fibrotic actions above and beyond reduced collagen I release (20, 21).

We hypothesize that TANGO1 is crucial for liver fibrogenesis through mediating secretion of procollagen I. Furthermore, we predict that in the absence of TANGO1, procollagen I would be retained in the ER leading to ER stress, induction of the UPR, and HSC apoptosis. Here, we show that collagen I secretion from HSCs is dependent on TANGO1 expression, and loss of TANGO1 leads to procollagen I retention in the ER which promotes UPR-mediated HSC apoptosis. Next, we uncovered a UPR signaling mechanism that upregulates TANGO1 expression in response to pro-fibrotic signals. Finally, we show that TANGO1 is critical for fibrogenesis in mice and is specifically upregulated in HSCs in response to pro-

fibrotic stimuli. Together, our work reveals a unique role for TANGO1 and the UPR in facilitating collagen I secretion and fibrogenesis.

Materials and Methods

HSC transfection and treatment

LX-2 cells or hHSCs were transfected with a siRNA against MIA3/TANGO1 (GE Dharmacon) using Oligofectamine (Invitrogen). For rescue experiments, the pcDNA3-GFP-TANGO1-PE plasmid, kindly provided by Dr. Vivek Malhotra (Centre for Genomic Regulation, Barcelona, Spain) or pcDNA-GFP-PE were transfected into LX-2 cells using Lipofectamine 3000 transfection reagent (Thermo Fisher) (10). 24hr post transfection, cells were serum starved for 4hr, followed by the indicated treatment. TGFβ was utilized at 10ng/mL for all experiments. For experiments involving 4-PBA (Sigma: 1716-12-7), serum starvation was performed in the presence of 10μM 4-PBA or vehicle.

Immunoblotting

Cells were lysed in a modified RIPA buffer (20mM HEPES pH 7.5, 0.5% DOC, 0.2% SDS, 150mM NaCl, 2mM EDTA, 1% Triton plus protease inhibitors) and centrifuged to remove cell debris. Lysates were denatured using 5× Lamelli buffer with DTT (conditioned media) or β-ME (whole cell lysate), boiled, resolved using SDS-PAGE, and transferred to nitrocellulose membrane. Membranes were blocked and incubated with primary antibodies overnight followed by an appropriate secondary antibody, and developed. Purchased primary antibodies are listed in supplemental methods. The antibody against TANGO1 was generated by Pacific Immunology as previously described (10). All experiments are representative of a minimum of three independent experiments with quantification and statistics performed using ImageJ and Prism respectively.

Confocal Microscopy

Cells were plated on fibronectin-coated wells, transfected, and treated with TGFβ or vehicle. Following treatment, cells were fixed in 4% paraformaldehyde, permeabilized in 0.1% Triton X-100 in PBS (except for Figures 1C and S1B), washed in PBS and blocked in 5% BSA in PBS. Cells were incubated with primary antibodies overnight at 4°C, followed by an appropriate fluorescently tagged secondary antibody. Antibodies were diluted in 5% BSA. DAPI was used to stain nuclei. All images were taken with a Zeiss LSM 5 Pascal (Germany) with the same laser intensity and power within each experiment. ImageJ was used to quantify the integrated density of each image and the RG2B plugin was used to quantify colocalization. Primary antibodies are outlined in supplemental methods or described above.

qPCR

After treatment, cells of liver tissue were harvested using Trizol and mRNA harvested using Qiagen RNeasy kit. Equal amounts of mRNA were converted into cDNA and qPCR was performed.

Apoptosis analysis

For TUNEL staining, the In Situ Cell Death Detection Kit, Fluorescein (Roche) was utilized. Cells were pretreated with 4-PBA or a vehicle in basal media where indicated, followed by treatment with TGFβ or a vehicle for 48hr. Cells were fixed and stained according to the manufacturer's protocol.

CCl_4 treatment and analysis of fibrosis

C57Bl/6J TANGO1$^{+/-}$ embryos were purchased from Mutant Mouse Resource Research Center at UC Davis (deposited by Genentech) and implanted into C57Bl/6J surrogate mothers. Mice were bred according to IACUC protocol and treatment groups consisted of littermates that were age and gender matched (n=5 for olive oil, n=6 for CCl_4 treatment). 0.5μl/mg CCl_4 was administered via intraperitoneal injection twice a week for 6 weeks. One day following the final injection, the mice were sacrificed and livers harvested. Fibrosis was analyzed by Sirius Red staining (paraffin-embedded tissues, IHC Bioworld), Hydroxyproline analysis, qPCR, immunoblotting, and immunofluorescence using protocols previously described (24). Protein lysates were harvested by homogenizing liver tissue in a modified RIPA buffer (50mM Tris-HCl, pH 7.4, 1% Triton X-100, 0.2% sodium deoxycholate, 0.2% sodium dodecylsulfate (SDS), 1mM EDTA). All experiments and procedures were performed in accordance with IACUC-approved protocols.

XBP-1 CRISPR and analysis

Lentiviral CRISPR plasmids against XBP1 were previously generated and packaged into HEK 293T cells (25). LX-2 cells were infected with lentivirus and cells were selected with 2ug/mL blastocidin. XBP1 knockout was confirmed by qPCR (25). To assess XBP1 splicing, mRNA was harvested from HSCs treated with TGFβ or vehicle, and underwent RT-PCR. The cDNA was purified, and PCR was performed using primers that span the spliced region of XBP1. The unspliced version of XBP1 contains a Pst1 restriction digest site, so the PCR product was digested with Pst1 for 1hr at 37°C and resolved on a 1.7% Agarose gel (25).

Supplemental Methods

Methods describing cell culture, qPCR primers, primary antibodies, viral packaging and infection, BDL, and the human biospecimens used are located in the supplementary material.

Results

TANGO1 contributes to collagen I secretion in HSCs

To identify proteins involved in procollagen I trafficking through the secretory pathway, we performed a targeted siRNA screen purchased from GE Dharmacon (Colorado, United States). We focused on collagen I secretion because it is the most highly expressed collagen isoform in HSCs and commonly implicated in cirrhosis (Figure S1A) (3). The screen consisted of siRNAs targeting 21 proteins involved in the secretory pathway. LX-2 cells were transfected with the siRNA and treated with TGFβ or a vehicle control for 24hr.

Conditioned media was harvested and collagen I secretion was examined using immunoblotting (Supplementary Table 1). Of the targets that were necessary for collagen I secretion (siRNA reduced collagen I secretion greater than 50% of control siRNA), the protein TANGO1 was of interest due to its previously reported specificity for collagen VII secretion in osteoblasts (10). Thus, we chose to focus on the role of TANGO1 in collagen secretion from HSCs.

TANGO1 mediates collagen I secretion from HSCs

LX-2 cells were transfected with a siRNA targeting TANGO1 (siTANGO1), which reduced TANGO1 protein levels to 32±15% of cells transfected with a control siRNA (siControl, Figure 1A). Following transfection, cells were treated with TGFβ, and collagen I secretion into the media was examined by immunoblot. As anticipated, collagen I secretion increased after TGFβ treatment in siControl cells, but both basal and TGFβ-stimulated collagen I secretion was significantly reduced in siTANGO1 cells (Figure 1B). Interestingly, this effect was specific to collagen I, as secretion of fibronectin, another matrix protein, was unaffected by loss of TANGO1. Collagen I secretion was also analyzed using confocal microscopy by staining non-permeabilized cells for collagen I. Extracellular collagen I was significantly decreased in siTANGO1 cells compared to siControl cells (Figure 1C). Reduced collagen I deposition was also observed in primary human HSCs (hHSCs, ScienCell) transfected with a siRNA against siTANGO1 (Figure S1B). To confirm the specificity of the siTANGO1 construct, we rescued TANGO1 expression using a pcDNA3-GFP-TANGO1-PE plasmid, kindly provided by Dr. Vivek Malhotra (Centre for Genomic Regulation, Barcelona, Spain). LX-2 cells were cotransfected with siTANGO1 and the TANGO1 plasmid or a control plasmid (Figure 1D, left panel). The cells were then treated with TGFβ or vehicle for 24hr and collagen secretion into the conditioned media was analyzed by immunoblotting (Figure 1D, right panel). Exogenous TANGO1 expression rescued collagen I secretion in siTANGO1 cells. Thus, these complementary knockdown and rescue experiments confirm that TANGO1 mediates collagen I secretion in HSCs.

Collagen I is retained in the ER upon loss of TANGO1

The impaired collagen I secretion led us to next examine if procollagen I was retained intracellularly in siTANGO1 cells. siControl or siTANGO1 cells were treated with vehicle or TGFβ, fixed, permeabilized, and co-stained for procollagen I and TANGO1. siTANGO1 cells displayed an increase in retained procollagen I in the presence of vehicle or TGFβ treatment compared to siControl cells (Figure 2A). To determine if the retained procollagen I localized within the ER, LX-2 cells were costained for procollagen I and one of two ER markers: ER chaperone protein disulfide-isomerase (PDI) or ERGIC53 (Figure 2B). The retained procollagen I colocalized with both PDI (top panel) and ERGIC53 (bottom panel), indicating that procollagen I is retained within the ER in the absence of TANGO1. Procollagen I retention within the ER was confirmed using Immunogold EM to visualize procollagen I (Figure S1C). In siControl cells treated with TGFβ, procollagen I can be visualized in the cytosol, likely in transport to the plasma membrane for secretion (denoted by the asterisk), but in siTANGO1 cells, procollagen I remains at the ER (arrows). As increased protein retention in the ER can lead to ER stress and induction of the UPR, we next examined ER morphology using TEM to examine if TANGO1 loss led to ER dilation or

fragmentation, hallmarks of ER stress. Both ER dilation and fragmentation were evident upon TANGO1 knockdown (Figure 2C). Together, this data indicates that upon loss of TANGO1 expression, procollagen I is retained within the ER and leads to ER stress.

Knockdown of TANGO1 induces the UPR and drives HSC apoptosis

Morphologic evidence of ER stress led us to next examine if the UPR was activated in siTANGO1 cells by analyzing downstream targets of the three UPR signaling pathways. hHSCs were transfected with siControl or siTANGO1 and treated with vehicle, TGFβ or tunicamycin (positive control) for matching time points. Immunoblotting revealed increased expression of the UPR marker BiP in siTANGO1 cells at basal conditions and this expression was further upregulated upon TGFβ treatment (Figure 3A). qPCR analysis also revealed significant induction of several UPR markers upon TANGO1 loss either at basal conditions or upon TGFβ treatment for 24hr. These markers include ERdj4, ER degradation enhancer mannosidase alpha (EDEM), PDI, BiP, ERp57, Derlin-3, Wolfram Syndrome 1 (WFS1), ERp72, and ATF4 (Figure 3B) (26–28). Gadd34 was the only marker tested which did not show increased expression in response to TANGO1 knockdown. Interestingly, we also noted increased expression of UPR markers erdj4, EDEM, PDI, BiP, and ERp72 in TGFβ treated control cells, indicating that TGFβ itself can drive some level of UPR signaling. Together, these data show that loss of TANGO1 leads to activation of the UPR, and that TANGO1 may prevent basal (or constitutive) ER stress.

Canonically, if ER stress is unresolved by the UPR, cells switch to a terminal phenotype and undergo UPR-mediated apoptosis. HSC apoptosis is critical to fibrosis resolution; thus we were interested in whether loss of TANGO1 could promote apoptosis in hHSCs. We first analyzed expression of CHOP and DR5 and found that both were upregulated in siTANGO1 cells, indicative of the UPR progressing to pro-apoptotic signaling (Figure 4A). We next studied the occurrence of hHSC apoptosis by examining caspase-3 cleavage. siTANGO1 cells exhibited increased caspase-3 cleavage at both basal conditions and in response to 24hr TGFβ treatment (Figure 4B). HSC death was confirmed using TUNEL staining, which revealed a higher percentage of TUNEL-positive cells in the absence of TANGO1 compared to Control cells at 48hr post treatment (Figure 4C). To determine if the observed apoptosis observed was a direct result of UPR signaling, we utilized two approaches. First, we pretreated siTANGO1 hHSCs with the chemical chaperone 4-PBA, which ameliorates ER stress, and observed a reduction of apoptosis to control levels (Figure 4C). Second, we analyzed the role of CHOP in siTANGO1-induced cell death, since CHOP is critical for the induction of apoptosis during prolonged ER stress. Primary HSCs were isolated from WT or CHOP knockout mice, transfected with siRNA against TANGO1 or a scrambled control, and treated with TGFβ or vehicle for 48hr. Upon TUNEL analysis, we observed that WT mice displayed increased apoptosis when TANGO1 expression was reduced, while $CHOP^{-/-}$ cells transfected with siTANGO1 displayed no increase in cell death (Figure 4D). These data show that TANGO1 loss leads to UPR-mediated apoptosis.

The elevated apoptosis in siTANGO1 hHSCs led us to question whether the observed defect of collagen I secretion in Figure 1 primarily occurred through a function of disrupted ER export or through HSC apoptosis. To address this issue, LX2 cells were infected with a

lentivirus encoding an shRNA against caspase-3 which ablates UPR-mediated apoptosis (Figure S2A). A scrambled shRNA served as a control. TANGO1 expression was subsequently reduced using an siRNA, and collagen I secretion into the conditioned media was analyzed. We found that reduced HSC apoptosis through silencing caspase-3 did not rescue the collagen I secretion defect, indicating that apoptosis is an effect, rather than a cause of impaired collagen I secretion (Figure S2B).

To examine whether loss of TANGO1 led to apoptosis of other liver cell types, we transfected immortalized hepatocytes (HepG2) with the siRNA against TANGO1. These cells exhibited a much attenuated apoptotic response compared to control cells, indicative of a cell-type specific response (Figure S3A). This may be due to less endogenous collagen I secretion by hepatocytes, as we also observed attenuation of apoptosis in siTANGO1 cells when procollagen I expression is concomitantly decreased using a shRNA targeting collagen1α1 (Figure S3B and C).

TANGO1 is a novel ER stress responsive protein

Previous studies have indicated that the UPR is activated during, and critical for, HSC activation (29, 30). We observed induction of the UPR control cells after TGFβ treatment, confirming that ER stress is present during HSC activation (Figure 3B). A key aspect of UPR signaling involves upregulation of proteins involved in ER export. The role of TANGO1 in procollagen I export, as well as the UPR activation upon TGFβ treatment led us to test whether the UPR upregulated TANGO1 expression. LX-2s were treated with TGFβ, tunicamycin, or a vehicle control, and TANGO1 expression was analyzed. TGFβ treatment induced TANGO1 expression two-fold, while tunicamycin treatment led to a larger four-fold increase in TANGO1 expression (Figure 5A). Furthermore, pretreatment with 4-PBA blocked both the TGFβ and tunicamycin induction of TANGO1, implicating that TANGO1 is upregulated downstream of the UPR. As we previously identified procollagen I retention as a key driver of UPR-mediated apoptosis when TANGO1 expression is reduced (Figure S3C), we next examined whether upregulation of procollagen I expression was directly responsible for increased TANGO1 expression. TANGO1 expression in response to TGFβ was attenuated in cells where procollagen Iα1 expression was reduced, implicating a role for increased procollagen I expression in driving the UPR and TANGO1 expression (Figure S3D).

These data led us to examine how the UPR mediates TANGO1 expression. The UPR regulates several transcription factors, so we analyzed the genomic region upstream of the gene that encodes TANGO1 using the programs TFBind and PROMO to predict transcription factor binding sites. We identified potential binding sites for the UPR-activated transcription factor XBP1. XBP1 is a transcription factor which is activated through splicing by phosphorylated IRE1, and translocates to the nucleus where it promotes gene expression. To examine whether XBP1 splicing occurs in response to TGFβ treatment, we used PCR to amplify XBP1 from cDNA, and digested the product with the restriction enzyme Pst1, as spliced XBP1 no longer contains a Pst1 digestion site (25). Indeed, we observed increased XBP1 splicing in TGFβ treated LX-2 cells (Figure 5B). We next utilized CRISPR-mediated knockout of XBP1 expression to generate two clonal LX-2 cell lines lacking XBP1

expression and a control cell line, and analyzed whether XBP1 regulates TANGO1 expression (Figure 5C)(25). Basal TANGO1 expression was reduced in XBP1 knockout cells, and there was little to no increase in TANGO1 following TGFβ treatment in either XBP-1 CRISPR cell line (Figure 5D). To confirm that TANGO1 function was similarly impaired, we analyzed collagen I secretion using immunoblotting. As expected, collagen I secretion, but not fibronectin secretion, was disrupted in the absence of XBP1 expression (Figure 5E). Together, these data show that XBP1 is critical for the UPR-mediated induction of TANGO1, facilitating procollagen I export from the ER upon HSC activation.

TANGO1 expression is upregulated in response to fibrogenic stimuli

The *in vitro* upregulation of TANGO1 in response to TGFβ led us to examine whether TANGO1 expression is increased in cirrhosis. Analysis of human liver biopsies revealed a significant increase in TANGO1 expression in cirrhotic compared to non-cirrhotic controls (Figure 6A). Increased TANGO1 expression was also observed in two separate mouse models of fibrosis, CCl_4 and BDL, compared to their respective controls (Figure 6B and C). Next, we examined whether TANGO1 expression was increased specifically in HSCs. hHSCs, immortalized LX-2 cells, hepatocytes (HepG2), sinusoidal cells (TSEC), and cholangiocytes (NH2) were treated with TGFβ for 24hrs and TANGO1 expression was analyzed using qPCR. LX-2 cells and hHSCs displayed a significant increase in TANGO1 (Figure 6D). HepG2 cells displayed a small but statistically significant increase in TANGO1 expression, but this was dramatically lower than the changes seen in LX-2 or hHSCs (1.2 fold in HepG2, 2.4 and 2.8 fold in LX-2 and hHSCs respectively). TSEC and NHC2 cells displayed no increase in TANGO1 expression upon TGFβ treatment. Increased TANGO1 expression in hHSCs following TGFβ was further confirmed using Western blot (Figure 6E). These data highlight a cell-type specific increase in TANGO1 expression in response to TGFβ.

TANGO1 is critical for fibrogenesis

Finally, we sought to determine whether TANGO1 is involved in liver fibrogenesis. TANGO1-null mice are embryonic lethal due to altered bone development, thus we utilized $TANGO1^{+/-}$ mice to assess whether a reduction in TANGO1 expression impacts fibrogenesis (11). $TANGO1^{+/-}$ mice displayed no obvious phenotypic differences prior to treatment, or altered collagen deposition in liver, muscle, or skin (Figure 7A olive oil, Figure S4). However, a bone defect was observed in adult $TANGO1^{+/-}$ mice, with decreased cortical thickness in the tibia compared to WT controls.

Cirrhosis was induced in $TANGO1^{+/-}$ or WT mice through intraperitoneal injections of 0.5mg CCl_4/kg twice a week for 6 weeks, after which livers were harvested and fibrogenesis was analyzed (24). Olive oil injection served as a vehicle control. Both Sirius Red staining and hydroxyproline analysis showed less fibrogenesis following CCl_4 injection in $TANGO1^{+/-}$ mice compared to WT littermates (Figures 7A and B). $TANGO1^{+/-}$ mice also displayed no significant increase in pro-fibrotic genes *col1α1, α-sma, timp1*, or *tgfβ1* after CCl_4 treatment (Figure 7C), or protein expression of α-SMA or PDGFRβ (Figure 7D). The reduced expression of procollagen I in $TANGO1^{+/-}$ mice seemed counterintuitive at first glance given that TANGO1 regulates collagen secretion rather than transcription. These

results suggest that increased retention of collagen I within the ER may drive HSC apoptosis or impaired HSC activation. To provide insight into this, we examined the number of HSCs within the liver using immunofluorescence to label HSCs through PDGFRβ or Desmin staining. We found a reduction in the number of PDGFRβ- and Desmin-positive cells in the livers from CCl_4-treated TANGO1$^{+/-}$ mice compared to WT mice. This indicates that the observed reduction in fibrogenesis at least in part results from a reduced population of HSCs that may occur through HSC apoptosis (Figure S5). Lastly, we confirmed the role of TANGO1$^{+/-}$ in fibrogenesis using a second mouse model, where WT or TANGO1 mice were subjected to BDL to induce fibrogenesis or a sham surgery. After three weeks, livers were harvested and analyzed for evidence of fibrosis. We found that TANGO1$^{+/-}$ mice that underwent BDL displayed less collagen deposition as analyzed by Sirius Red staining or hydroxyproline assay compared to WT controls (Figure S6A and B), and lower expression of the fibrotic markers *col1α1, α-sma, timp1*, and *fibronectin*.(Figure S6C). In total these studies recapitulate the importance of TANGO1 in mediating fibrogenesis both *in vivo* and *in vitro*.

Discussion

Previous studies on fibrosis often focused on mechanisms of procollagen I gene expression and matrix dynamics during fibrogenesis (31). Conversely, details on the intracellular trafficking of procollagen I are lacking. This study identifies TANGO1 as a novel mediator of liver fibrosis by virtue of its ability to facilitate procollagen I processing and secretion in HSCs. We show for the first time that TANGO1 is critical for collagen I secretion in HSCs, and that loss of TANGO1 drives HSC apoptosis due to an inability of the cell to clear retained procollagen I from the ER. Furthermore, HSC activation induces TANGO1 expression, a mechanism which requires the UPR-regulated transcription factor XBP1. Thus, TANGO1 and the UPR are critical for collagen I secretion and HSC survival during HSC activation. Finally, we identify TANGO1 as a critical mediator of fibrogenesis *in vivo* (Figure 8).

ER stress is involved in numerous disease states, including liver diseases such as NAFLD, NASH, and Alpha-1 antitrypsin deficiency (14, 32). These diseases exhibit ER stress in hepatocytes, leading to parenchymal cell death and subsequent inflammation and fibrosis; however, the role of ER stress in HSCs during fibrogenesis is less understood. Only recently was the physiologic importance of ER stress in HSCs identified, with UPR signaling as profibrogenic: critical for increased α-SMA expression and upregulation of Smad-2 (29, 30, 33). ER stress is also implicated in idiopathic pulmonary fibrosis, where activation of lung fibroblasts by TGFβ was dependent upon UPR activation (34). Here we identify UPR signaling to be critical for another key aspect of HSC activation: collagen I secretion. Thus, ER stress and induction of the UPR appear to be critical for the active secretory function of myofibroblasts. Our work highlights how upregulation of TANGO1 by the UPR prevents constitutive ER stress in HSCs by meeting the secretory demands of increased procollagen I production.

A critical role of the UPR is upregulation of proteins involved in the folding and trafficking of proteins through the secretory pathway. We initially observed UPR induction and HSC

apoptosis in the absence of TANGO1, but also found that TANGO1 expression increased upon tunicamycin treatment. These data led us to hypothesize that TANGO1 expression is mediated by the UPR to facilitate clearance of procollagen I from the ER. Upon further investigation, we found that pretreatment of HSCs with the chemical chaperone 4-PBA ameliorated TGFβ- or tunicamycin-induced TANGO1 expression, and similar results were observed when procollagen I expression was blocked using an shRNA. Finally, we uncovered the mechanism of TANGO1 induction involved XBP1 as cells lacking XBP1 displayed no increase in TANGO1 expression following TGFβ treatment. Together, this data outlines a well-orchestrated mechanism by which HSCs are able to accommodate TGFβ-mediated procollagen I folding and trafficking via UPR signaling and subsequent upregulation of TANGO1, which in turn promotes collagen I exit from the ER.

The UPR may play an anti-fibrotic role in HSCs as well. Elimination of activated myofibroblasts is critical for fibrosis regression (35). One mechanism by which this can occur is HSC apoptosis (20, 21, 36). Induced non-physiologic ER stress in HSCs was shown to be anti-fibrotic, due to induction of cell death in cultured HSCs (20, 37, 38). We observed increased UPR signaling in siTANGO1 cells, and increased expression of CHOP and DR5, genes involved in UPR-mediated apoptosis. This prompted us to assess whether loss of TANGO1 in HSCs led to increased apoptosis. Both TUNEL staining and caspase-3 cleavage were increased in siTANGO1 cells, and these effects were exacerbated by TGFβ treatment. Furthermore, this apoptosis was a direct result of UPR signaling, as both pretreatment with 4-PBA or loss of CHOP expression blocked HSC death in siTANGO1 cells. It is interesting to note the significant occurrence of apoptosis upon knockdown of TANGO1, even in the absence of TGFβ treatment and HSC activation. We hypothesize that even quiescent HSCs require TANGO1 expression to mediate basal levels of collagen I secretion, and this is not restricted to cell lines, as the primary mouse HSCs in Figure 4D display the same phenotype. Furthermore, quiescent HSCs express significantly higher levels of collagen I than hepatocytes at basal conditions, potentially explaining why loss of TANGO1 drives apoptosis of quiescent HSCs, but not hepatocyte apoptosis (39). These findings indicate that while TANGO1 is crucial for accommodating increased procollagen I export from the ER, disruption of this process disrupts cellular homeostasis and drives apoptosis.

TANGO1 has previously been identified as an ER-localized protein involved in procollagen VII export from the ER in chondrocytes (10). TANGO1 is predicted to serve this role by recruiting procollagen VII, cytosolic proteins, and ER-Golgi intermediate compartment (ERGIC) vesicles to ER exit sites and facilitating the formation of large ER export vesicles that accommodate procollagen VII fibrils (40, 41). We find a role for TANGO1 in selectively mediating collagen I secretion from HSCs, with loss of TANGO1 disrupting ER export of procollagen I, but not fibronectin. Interestingly, previous work in keratinocytes (that express procollagen VII) and fibroblasts (that primarily express procollagen I) found no alterations in collagen I secretion *in vitro*; whereas *in vivo* depletion of TANGO1 affected secretion of several collagen isoforms from chondrocytes and fibroblasts, including both collagen I and collagen VII (10). This difference between HSCs and chondrocytes, as well as the differential effects of TANGO1 loss between HSCs and HepG2 cells observed in this study, may arise from the selective expression of TANGO1 isoforms. TANGO1 homologues such as MIA1, MIA2, and OTOR display restricted expression profiles, primarily expressed in

chondrocytes, hepatocytes, and cochlea respectively (42–44). More research is needed to fully understand the specificity of TANGO isoforms in collagen secretion from different cell types.

Anti-fibrotic therapies that specifically target activated HSCs are critical to limit fibrogenesis and promote fibrosis regression. A goal for fibrosis treatment is to specifically drive apoptosis of HSCs to disrupt fibrogenesis while limiting damage to hepatocytes and other liver cells. Thus, we propose TANGO1 inhibition as an attractive target for anti-fibrotic therapies. In conclusion, these data provide novel insight into the mechanisms of procollagen I trafficking and fibrogenesis, and lay the framework for future studies to identify targets for treating liver disease.

Supplementary Material

Refer to Web version on PubMed Central for supplementary material.

Acknowledgments

Financial Support: Supported by National Institutes of Health (NIH), USA R01 DK59615 and R01 AA21171 (VHS), DK100575 (RCH) DK97178 (HM), T32 (DK07198) and American Liver Foundation (JLM)

We would like to thank the generous support of the Mayo Clinic Center for Cell Signaling (P30DK084567), in particular the Clinical Core and the Optical Microscopy Core for their support. We also thank the Biomaterials and Histomorphometry Core and the Electron Microscopy Core at Mayo Clinic and Dr. Bing Huang for his help. Finally, we thank Dr. Vivek Malhotra and David Katzmann for reagents and support.

Abbreviations

HSCs	Hepatic Stellate Cells
ER	Endoplasmic Reticulum
UPR	Unfolded Protein Response
PDI	Protein Disulfide Isomerase
TANGO1	Transport And Golgi Organization 1
IRE-1	inositol–requiring enzyme-1
ATF6	activating transcription factor 6
PERK	protein kinase RNA-like ER kinase
XBP1	X-Box Binding Protein 1
ATF4	activating transcription factor 4
CCl_4	carbon tetrachloride
TGFβ	transforming growth factor β
Veh	Vehicle

Tuni	Tunicamycin
4-PBA	4-phenylbuterate
ERGIC	ER-Golgi intermediate compartment
EDEM	ER degradation enhancer mannosidase alpha
WFS1	Wolfram Syndrome 1
BDL	Bile duct ligation

References

1. Friedman SL, Sheppard D, Duffield JS, Violette S. Therapy for fibrotic diseases: nearing the starting line. Science translational medicine. 2013; 5:167sr161.
2. Kocabayoglu P, Friedman SL. Cellular basis of hepatic fibrosis and its role in inflammation and cancer. Frontiers in bioscience. 2013; 5:217–230.
3. Lee UE, Friedman SL. Mechanisms of hepatic fibrogenesis. Best practice & research. Clinical gastroenterology. 2011; 25:195–206. [PubMed: 21497738]
4. Iwaisako K, Jiang C, Zhang M, Cong M, Moore-Morris TJ, Park TJ, Liu X, et al. Origin of myofibroblasts in the fibrotic liver in mice. Proceedings of the National Academy of Sciences of the United States of America. 2014; 111:E3297–E3305. [PubMed: 25074909]
5. Chessler SD, Byers PH. BiP binds type I procollagen pro alpha chains with mutations in the carboxyl-terminal propeptide synthesized by cells from patients with osteogenesis imperfecta. The Journal of biological chemistry. 1993; 268:18226–18233. [PubMed: 8349698]
6. Ferreira LR, Norris K, Smith T, Hebert C, Sauk JJ. Association of Hsp47, Grp78, and Grp94 with procollagen supports the successive or coupled action of molecular chaperones. Journal of cellular biochemistry. 1994; 56:518–526. [PubMed: 7890810]
7. Wilson R, Lees JF, Bulleid NJ. Protein disulfide isomerase acts as a molecular chaperone during the assembly of procollagen. The Journal of biological chemistry. 1998; 273:9637–9643. [PubMed: 9545296]
8. Malhotra V, Erlmann P. Protein export at the ER: loading big collagens into COPII carriers. The EMBO journal. 2011; 30:3475–3480. [PubMed: 21878990]
9. Bard F, Casano L, Mallabiabarrena A, Wallace E, Saito K, Kitayama H, Guizzunti G, et al. Functional genomics reveals genes involved in protein secretion and Golgi organization. Nature. 2006; 439:604–607. [PubMed: 16452979]
10. Saito K, Chen M, Bard F, Chen S, Zhou H, Woodley D, Polischuk R, et al. TANGO1 facilitates cargo loading at endoplasmic reticulum exit sites. Cell. 2009; 136:891–902. [PubMed: 19269366]
11. Wilson DG, Phamluong K, Li L, Sun M, Cao TC, Liu PS, Modrusan Z, et al. Global defects in collagen secretion in a Mia3/TANGO1 knockout mouse. The Journal of cell biology. 2011; 193:935–951. [PubMed: 21606205]
12. Welihinda AA, Tirasophon W, Kaufman RJ. The cellular response to protein misfolding in the endoplasmic reticulum. Gene expression. 1999; 7:293–300. [PubMed: 10440230]
13. Rutkowski DT, Kaufman RJ. A trip to the ER: coping with stress. Trends in cell biology. 2004; 14:20–28. [PubMed: 14729177]
14. Malhi H, Kaufman RJ. Endoplasmic reticulum stress in liver disease. Journal of hepatology. 2011; 54:795–809. [PubMed: 21145844]
15. Calfon M, Zeng H, Urano F, Till JH, Hubbard SR, Harding HP, Clark SG, et al. IRE1 couples endoplasmic reticulum load to secretory capacity by processing the XBP-1 mRNA. Nature. 2002; 415:92–96. [PubMed: 11780124]
16. Gao Y, Sartori DJ, Li C, Yu QC, Kushner JA, Simon MC, Diehl JA. PERK is required in the adult pancreas and is essential for maintenance of glucose homeostasis. Molecular and cellular biology. 2012; 32:5129–5139. [PubMed: 23071091]

17. Lipson KL, Fonseca SG, Ishigaki S, Nguyen LX, Foss E, Bortell R, Rossini AA, et al. Regulation of insulin biosynthesis in pancreatic beta cells by an endoplasmic reticulum-resident protein kinase IRE1. Cell metabolism. 2006; 4:245–254. [PubMed: 16950141]

18. Scheuner D, Kaufman RJ. The unfolded protein response: a pathway that links insulin demand with beta-cell failure and diabetes. Endocrine reviews. 2008; 29:317–333. [PubMed: 18436705]

19. Lu M, Lawrence DA, Marsters S, Acosta-Alvear D, Kimmig P, Mendez AS, Paton AW, et al. Cell death. Opposing unfolded-protein-response signals converge on death receptor 5 to control apoptosis. Science. 2014; 345:98–101. [PubMed: 24994655]

20. De Minicis S, Candelaresi C, Agostinelli L, Taffetani S, Saccomanno S, Rychlicki C, Trozzi L, et al. Endoplasmic Reticulum stress induces hepatic stellate cell apoptosis and contributes to fibrosis resolution. Liver international : official journal of the International Association for the Study of the Liver. 2012; 32:1574–1584. [PubMed: 22938186]

21. Iredale JP, Benyon RC, Pickering J, McCullen M, Northrop M, Pawley S, Hovell C, et al. Mechanisms of spontaneous resolution of rat liver fibrosis. Hepatic stellate cell apoptosis and reduced hepatic expression of metalloproteinase inhibitors. The Journal of clinical investigation. 1998; 102:538–549. [PubMed: 9691091]

22. Mederacke I, Dapito DH, Affo S, Uchinami H, Schwabe RF. High-yield and high-purity isolation of hepatic stellate cells from normal and fibrotic mouse livers. Nature protocols. 2015; 10:305–315. [PubMed: 25612230]

23. Huebert RC, Jagavelu K, Liebl AF, Huang BQ, Splinter PL, LaRusso NF, Urrutia RA, et al. Immortalized liver endothelial cells: a cell culture model for studies of motility and angiogenesis. Laboratory investigation; a journal of technical methods and pathology. 2010; 90:1770–1781. [PubMed: 20644520]

24. Cao S, Yaqoob U, Das A, Shergill U, Jagavelu K, Huebert RC, Routray C, et al. Neuropilin-1 promotes cirrhosis of the rodent and human liver by enhancing PDGF/TGF-beta signaling in hepatic stellate cells. The Journal of clinical investigation. 2010; 120:2379–2394. [PubMed: 20577048]

25. Kakazu E, Mauer AS, Yin M, Malhi H. Hepatocytes release ceramide-enriched pro-inflammatory extracellular vesicles in an IRE1alpha-dependent manner. Journal of lipid research. 2016; 57:233–245. [PubMed: 26621917]

26. Todd DJ, McHeyzer-Williams LJ, Kowal C, Lee AH, Volpe BT, Diamond B, McHeyzer-Williams MG, et al. XBP1 governs late events in plasma cell differentiation and is not required for antigen-specific memory B cell development. The Journal of experimental medicine. 2009; 206:2151–2159. [PubMed: 19752183]

27. Wu J, Rutkowski DT, Dubois M, Swathirajan J, Saunders T, Wang J, Song B, et al. ATF6alpha optimizes long-term endoplasmic reticulum function to protect cells from chronic stress. Developmental cell. 2007; 13:351–364. [PubMed: 17765679]

28. Yu B, Wen L, Xiao B, Han F, Shi Y. Single Prolonged Stress induces ATF6 alpha-dependent Endoplasmic reticulum stress and the apoptotic process in medial Frontal Cortex neurons. BMC neuroscience. 2014; 15:115. [PubMed: 25331812]

29. Hernandez-Gea V, Hilscher M, Rozenfeld R, Lim MP, Nieto N, Werner S, Devi LA, et al. Endoplasmic reticulum stress induces fibrogenic activity in hepatic stellate cells through autophagy. Journal of hepatology. 2013; 59:98–104. [PubMed: 23485523]

30. Koo JH, Lee HJ, Kim W, Kim SG. Endoplasmic Reticulum Stress in Hepatic Stellate Cells Promotes Liver Fibrosis via PERK-Mediated Degradation of HNRNPA1 and Up-regulation of SMAD2. Gastroenterology. 2016; 150:181–193. e188. [PubMed: 26435271]

31. Mehal WZ, Schuppan D. Antifibrotic therapies in the liver. Seminars in liver disease. 2015; 35:184–198. [PubMed: 25974903]

32. Duwaerts CC, Maher JJ. Mechanisms of Liver Injury in Non-Alcoholic Steatohepatitis. Current hepatology reports. 2014; 13:119–129. [PubMed: 25045618]

33. Heindryckx F, Binet F, Ponticos M, Rombouts K, Lau J, Kreuger J, Gerwins P. Endoplasmic reticulum stress enhances fibrosis through IRE1alpha-mediated degradation of miR-150 and XBP-1 splicing. EMBO molecular medicine. 2016; 8:729–744. [PubMed: 27226027]

34. Baek HA, Kim do S, Park HS, Jang KY, Kang MJ, Lee DG, Moon WS, et al. Involvement of endoplasmic reticulum stress in myofibroblastic differentiation of lung fibroblasts. American journal of respiratory cell and molecular biology. 2012; 46:731–739. [PubMed: 21852685]
35. Kisseleva T, Brenner DA. Hepatic stellate cells and the reversal of fibrosis. Journal of gastroenterology and hepatology. 2006; 21(Suppl 3):S84–S87. [PubMed: 16958681]
36. Elsharkawy AM, Oakley F, Mann DA. The role and regulation of hepatic stellate cell apoptosis in reversal of liver fibrosis. Apoptosis : an international journal on programmed cell death. 2005; 10:927–939. [PubMed: 16151628]
37. Kawasaki K, Ushioda R, Ito S, Ikeda K, Masago Y, Nagata K. Deletion of the collagen-specific molecular chaperone Hsp47 causes endoplasmic reticulum stress-mediated apoptosis of hepatic stellate cells. The Journal of biological chemistry. 2015; 290:3639–3646. [PubMed: 25525267]
38. Sharma S, Mells JE, Fu PP, Saxena NK, Anania FA. GLP-1 analogs reduce hepatocyte steatosis and improve survival by enhancing the unfolded protein response and promoting macroautophagy. PloS one. 2011; 6:e25269. [PubMed: 21957486]
39. Friedman SL. Cellular sources of collagen and regulation of collagen production in liver. Seminars in liver disease. 1990; 10:20–29. [PubMed: 2186486]
40. Santos AJ, Raote I, Scarpa M, Brouwers N, Malhotra V. TANGO1 recruits ERGIC membranes to the endoplasmic reticulum for procollagen export. eLife. 2015; 4
41. Saito K, Yamashiro K, Ichikawa Y, Erlmann P, Kontani K, Malhotra V, Katada T. cTAGE5 mediates collagen secretion through interaction with TANGO1 at endoplasmic reticulum exit sites. Molecular biology of the cell. 2011; 22:2301–2308. [PubMed: 21525241]
42. Bosserhoff AK, Kaufmann M, Kaluza B, Bartke I, Zirngibl H, Hein R, Stolz W, et al. Melanoma-inhibiting activity, a novel serum marker for progression of malignant melanoma. Cancer research. 1997; 57:3149–3153. [PubMed: 9242442]
43. Robertson NG, Heller S, Lin JS, Resendes BL, Weremowicz S, Denis CS, Bell AM, et al. A novel conserved cochlear gene, OTOR: identification, expression analysis, and chromosomal mapping. Genomics. 2000; 66:242–248. [PubMed: 10873378]
44. Bosserhoff AK, Moser M, Scholmerich J, Buettner R, Hellerbrand C. Specific expression and regulation of the new melanoma inhibitory activity-related gene MIA2 in hepatocytes. The Journal of biological chemistry. 2003; 278:15225–15231. [PubMed: 12586826]

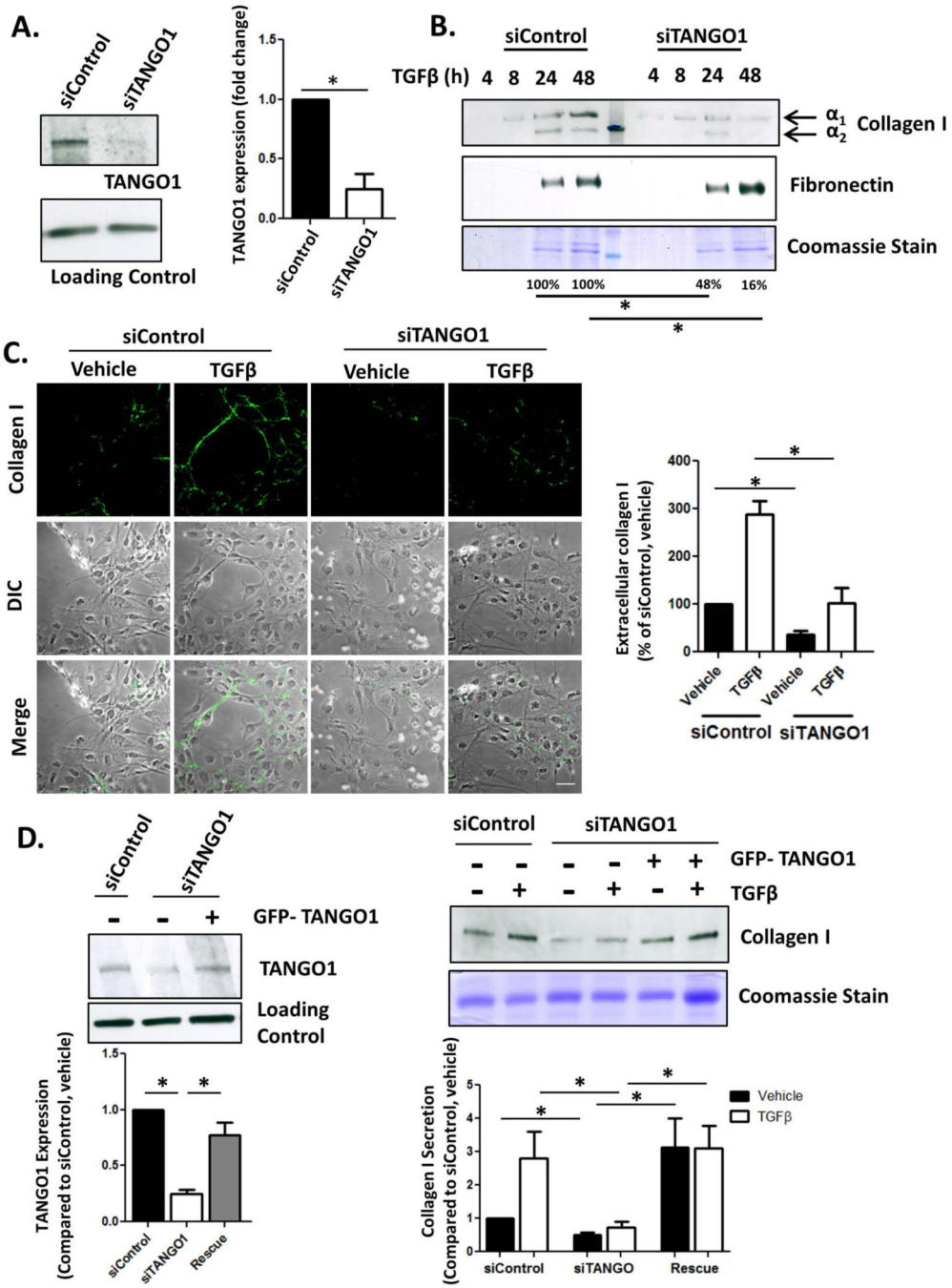

Figure 1. TANGO1 is critical for collagen I secretion from HSCs

A. LX-2 cells were transfected with an siRNA against TANGO1 (siTANGO1) or a scrambled Control (siControl). 72hrs after transfection, TANGO1 expression was analyzed by Western Blot with HSC70 serving as a loading control (quantification in the adjacent graph, *=p<0.05). B. siControl or siTANGO1 LX-2 cells were treated with 10ng/mL TGFβ or a vehicle control for 24hrs. Conditioned media was harvested, separated via SDS-PAGE, and collagen I and fibronectin levels were analyzed using immunoblotting (upper panel, *=p<0.05). Coomassie stain was used to confirm equal loading between siControl and

siTANGO1 pairs since conditioned media was harvested at different time points (lower panel). Quantification is displayed below the blots, n=4, *=p<0.05. C. Confocal images were taken of extracellular collagen I deposition by siControl or siTANGO1 LX-2 cells treated with vehicle or TGFβ. Cells were fixed but not permeabilized in order to eliminate staining for intracellular procollagen I. Pixel intensity was determined using ImageJ, adjusted for cell number, and is displayed in the adjacent graph. (Scale bar=50μm, n=4, *=p<0.001). D. LX-2 cells were cotransfected with an siRNA against TANGO1 (or control siRNA) and a plasmid expressing exogenous TANGO1 (or a control plasmid) for 48 hours followed by TGFβ treatment for 24hr. Whole cell lysate (Left Panel) was harvested and immunoblotted for TANGO1 and HSC70 (Loading Control). Conditioned media was also harvested, separated by SDS-PAGE and collagen I secretion was examined by immunoblotting (Right Panel). Coomassie staining confirmed equal loading. N=5, *=p<0.05.

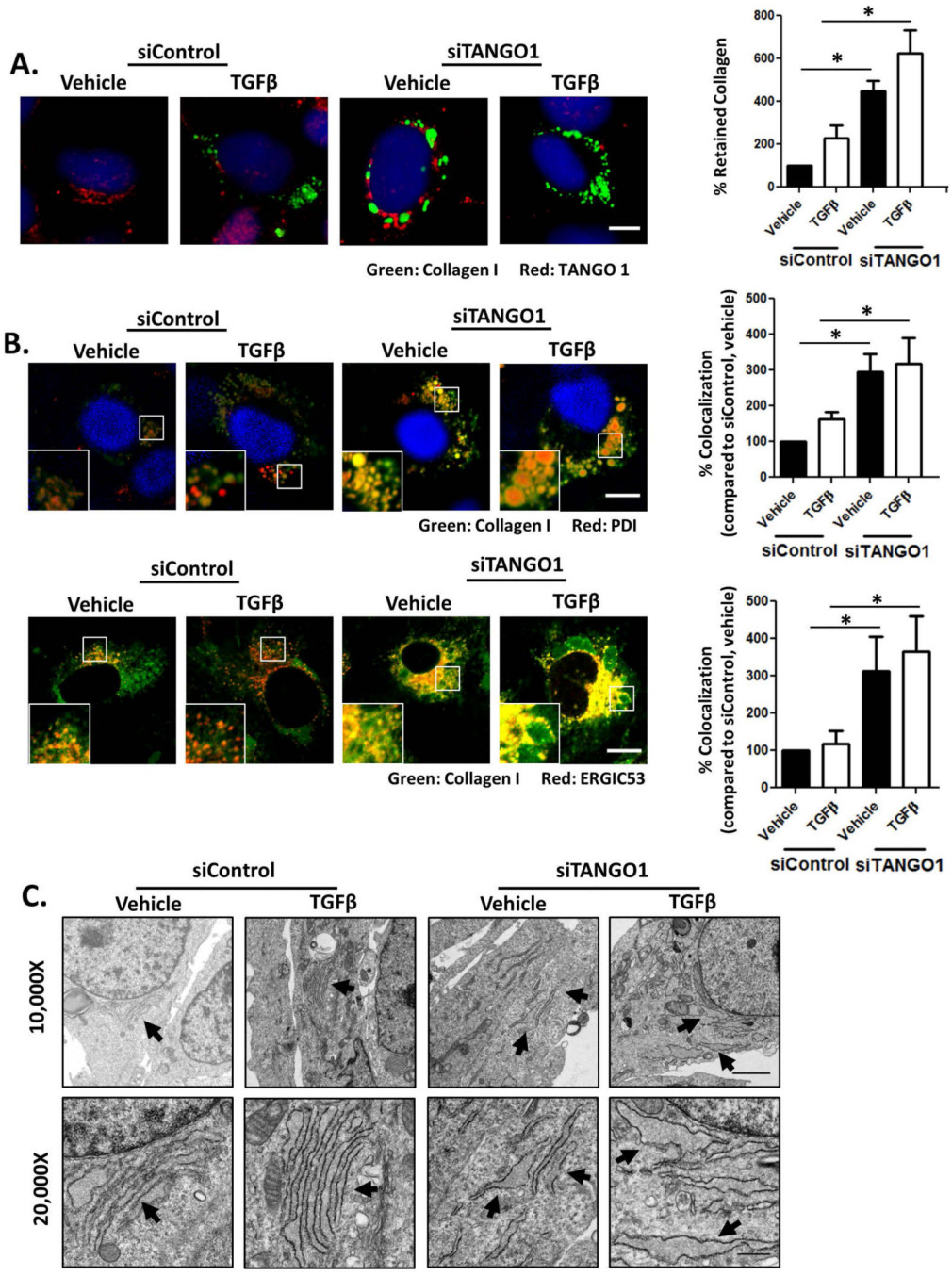

Figure 2. Procollagen I is retained in the ER in the absence of TANGO1 expression

A. siControl and siTANGO1 hHSCs were treated with TGFβ or a vehicle control, fixed, permeabilized, and costained for procollagen I and TANGO1. Procollagen I retention was analyzed by ImageJ and densitometry is displayed in the adjacent graph (Scale bar=10um, n=4, *=p<0.05). B: Confocal images of hHSCs transfected with siControl or siTANGO1 and treated with vehicle or TGFβ. Cells were fixed, permeabilized, and costained for procollagen I and PDI (upper panel) or procollagen I and ERGIC53 (lower panel). Colocalization of procollagen I with either PDI or ERGIC53 were analyzed by ImageJ and displayed in the

adjacent graphs (Scale bar=10μm, n=4, *=p<0.05) C. Electron microscopy was performed on siControl and siTANGO1 hHSCs treated with TGFβ or vehicle. siControl hHSCs displayed intact EM, whereas siTANGO1 hHSCs displayed distended and fragmented ER (For 10,000× magnification, scale bar = 2μm; for 20,000× magnification, scale bar=0.5μm).

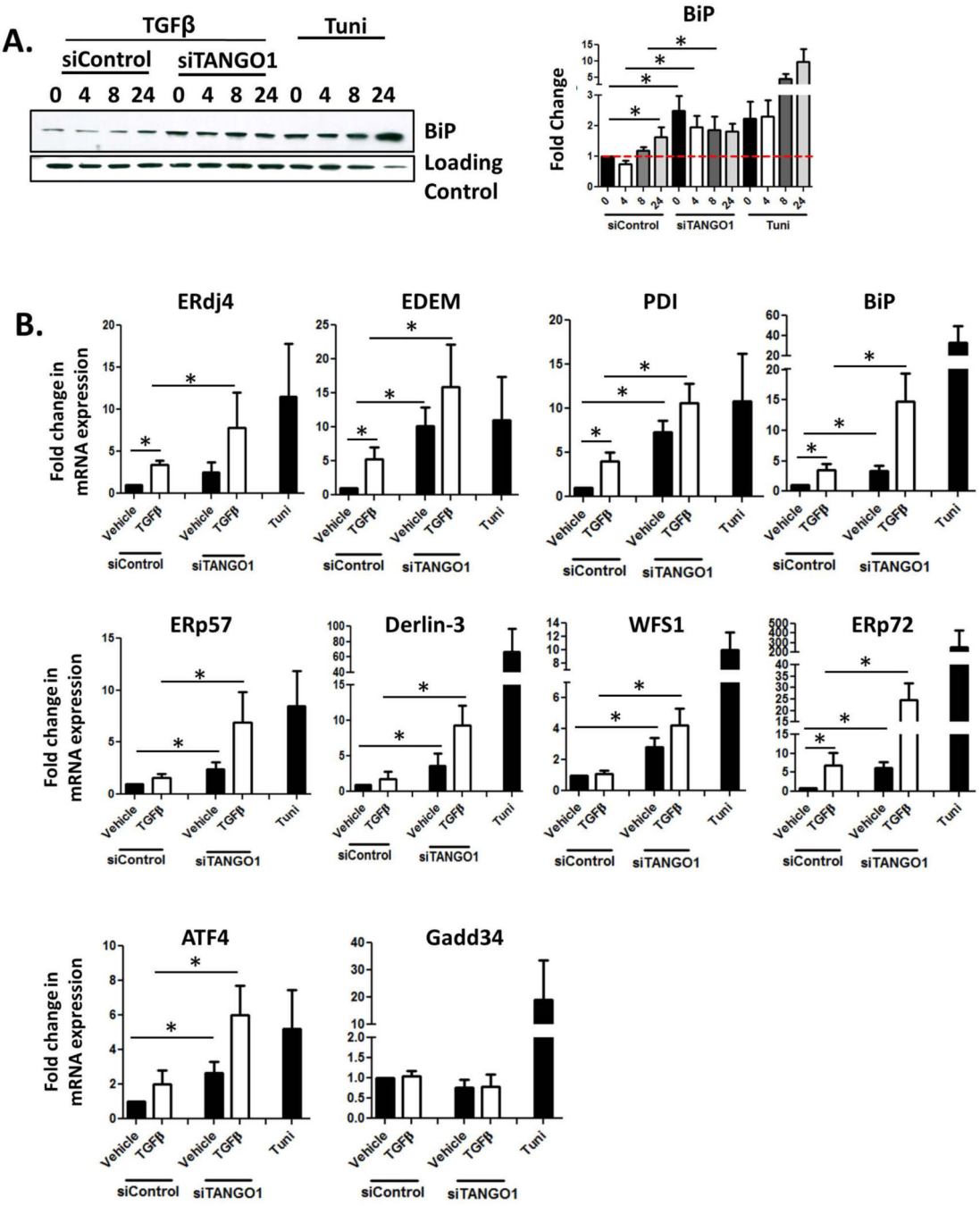

Figure 3. TANGO1 knockdown leads to UPR induction

Induction of the UPR was assessed using a combination of immunoblotting and qPCR to examine the expression of numerous downstream effectors. A. siTANGO1 or siControl hHSCs were treated with TGFβ for 0, 4, 8, or 24hrs. siControl cells were treated with tunicamycin for matching time points to serve as a positive control. Cells were lysed, separated by SDS-PAGE, and the UPR marker BiP was analyzed by immunoblot. HSC70 served as a loading control. Blots are representative of 4 separate experiments and quantification is located in the adjacent panel (n=6, *=p<0.05). The red dashed line

represents baseline expression (siControl, 0hr). B. Expression of UPR markers ERdj4, ERp57, Derlin-3, EDEM, BiP, WFS1, ERp72, Gadd34, PDI, and ATF4 in siControl or siTANGO1 hHSCs were analyzed by qPCR following 24hr treatment with vehicle or TGFβ. Tunicamycin treatment served as a positive control. N=5, *=$p<0.05$.

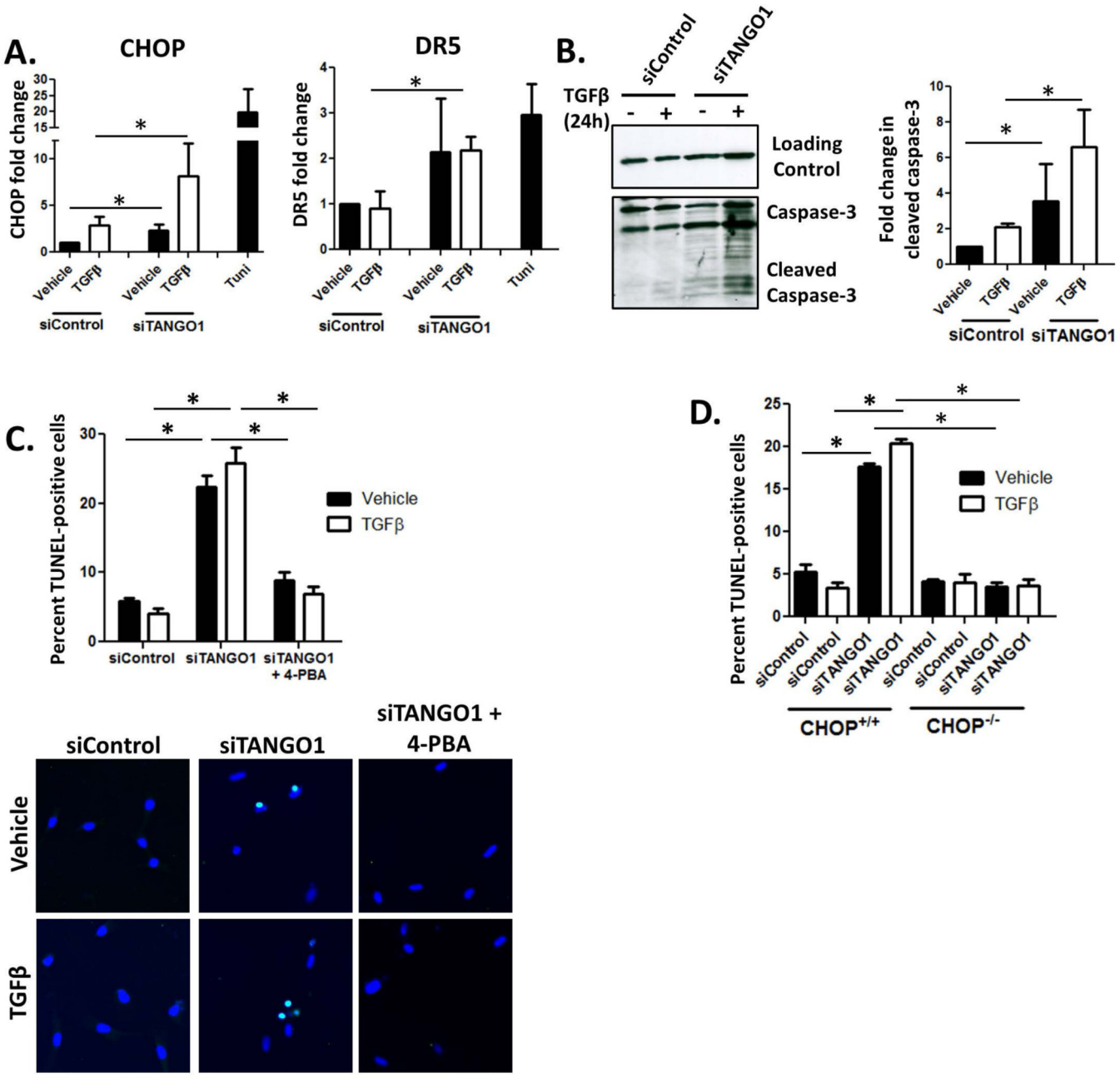

Figure 4. TANGO1 loss drives UPR-mediated HSC apoptosis

A. Activation of pro-apoptotic UPR signaling in hHSCs was examined by qPCR analysis of CHOP and DR5 expression. Cells were transfected with siRNA against TANGO1 or a scrambled control, and treated with TGFβ or vehicle (CHOP n=6, DR5 n=4, *=p<0.05). Tunicamycin treatment serves as a positive control. B. Caspase-3 cleavage was examined as a marker of apoptosis in siControl or siTANGO1 cells treated with TGFβ or a vehicle control. Levels of cleaved caspase-3 were quantified using ImageJ and displayed in the adjacent graph (n=3, *=p<0.05). C. Cell death was examined using the In Situ Cell Death Detection Kit from Roche. hHSCs were transfected with siControl or siTANGO1, treated with vehicle or TGFβ, with or without the chemical chaperone 4-PBA. Cells were fixed and

treated according to the manufacturer's protocol. DAPI was used to stain nuclei, with apoptotic cells costained with DAPI and the TUNEL reagent. The percent of TUNEL-positive cells from 4 separate experiments we quantified and representative images are shown. N=4, *=$p<0.001$. D. Primary HSCs were isolated from CHOP$^{-/-}$ mice or wild-type littermates, transfected with siTANGO1 or a control siRNA, treated with TGFβ or vehicle, and analyzed via TUNEL assay as described in Figure 6C. (n=3, *=$p<0.05$).

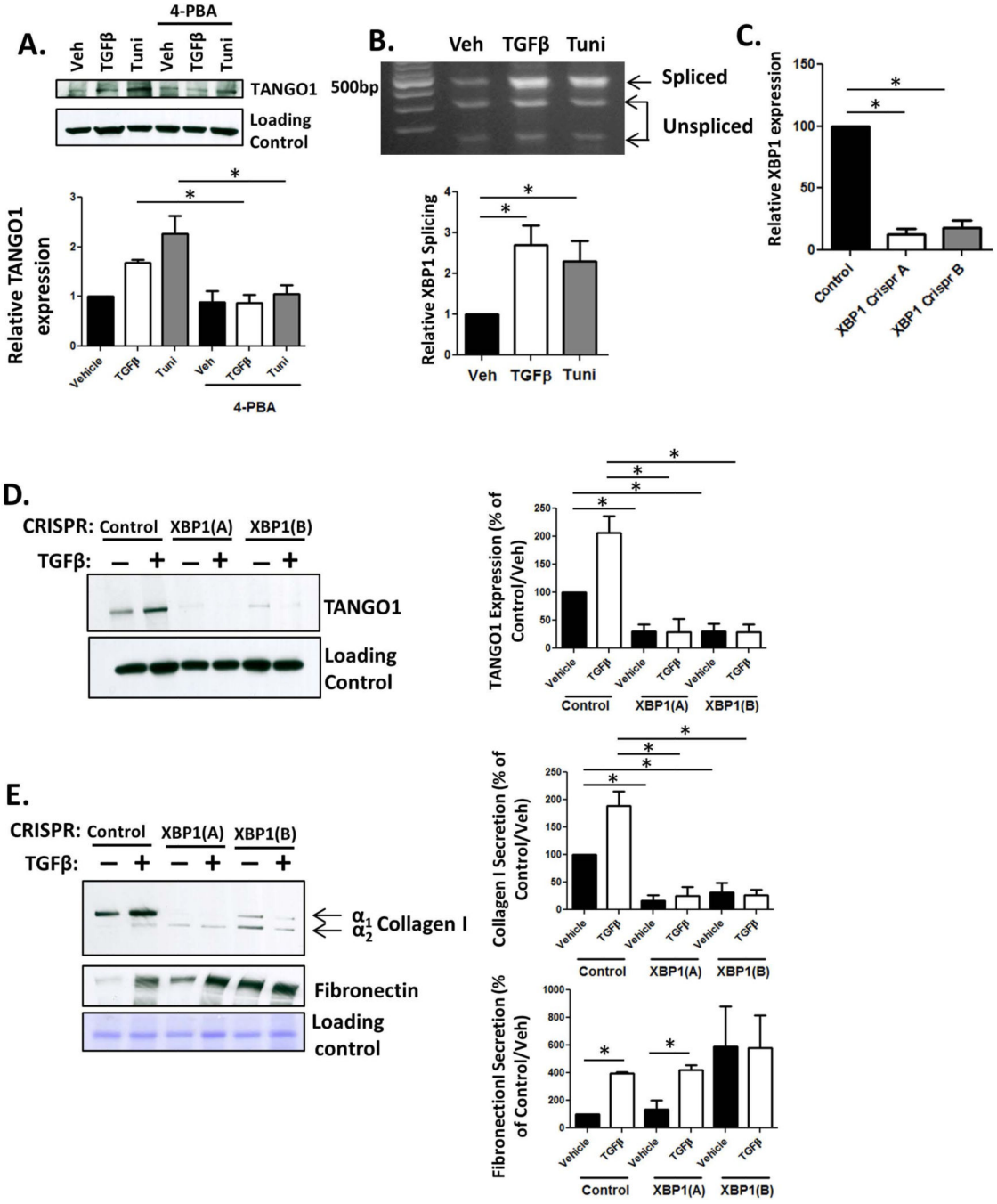

Figure 5. The UPR drives expression of TANGO1

A. siTANGO1 or siControl transfected LX-2 cells were serum starved in basal media containing 4-PBA or a vehicle for 4hr, followed by treatment with TGFβ or tunicamycin (Tuni) for 24hr. After treatment, cells were harvested, lysed, and analyzed for TANGO1 expression by immunoblotting. Quantification is displayed below (n=4, *=p<0.01). B. hHSCs were treated with vehicle or TGFβ and analyzed for XBP1 cleavage. Unspliced XBP1 is digested into two fragments (290bp and 183bp) and spliced XBP1 is visualized at 473b. Quantification located below, n=5, *=p<0.001. C. LX-2 cells were stably infected with

virus expressing one of two CRISPR constructs (A or B) targeting XBP1 or a control construct. XBP1 expression was analyzed by qPCR. D and E. Cells lacking XBP1 or control cells were treated with TGFβ or vehicle, and TCL and conditioned media were harvested. TANGO1 expression (TCL, D, n=3, *=p<0.01) and collagen I or fibronectin secretion (conditioned media, E, n=4, *=p,0.05) were measured using immunoblotting, following by ImageJ analysis in the adjacent graphs.

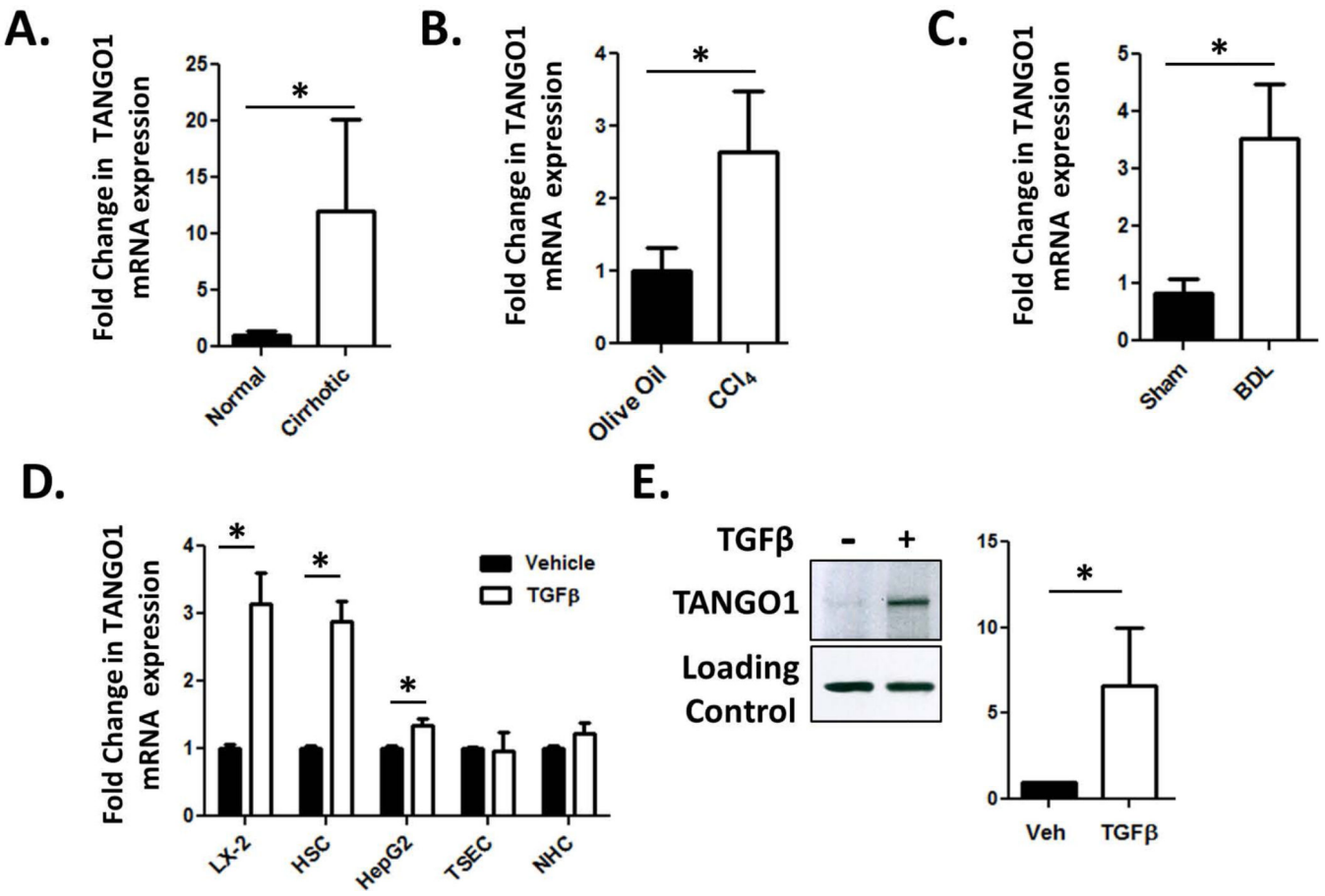

Figure 6. Profibrotic stimuli induce TANGO1 expression specifically in HSCs

A. mRNA was harvested from cirrhotic and non-cirrhotic human livers and TANGO1 levels were analyzed by qPCR (9 samples per group, *p<0.05). B and C. Livers were harvested from C57Bl/6J mice that either were treated with CCl_4 (or olive oil as a control) or underwent BDL (or a sham surgery). At sacrifice, mRNA was harvested from whole livers and analyzed for TANGO1 mRNA levels by PCR. *=p<0.05. D. Immortalized liver cells (LX-2, HepG2, TSEC, or NHC2) or primary human HSCs were treated with 10ng/ml TGFβ for 24hrs, after which mRNA was extracted and TANGO1 expression was analyzed by qPCR (n=4). *=p<0.01 D. HSCs were treated with TGFβ and analyzed for TANGO1 protein expression by immunoblot (quantification below). n=6, *=p<0.05.

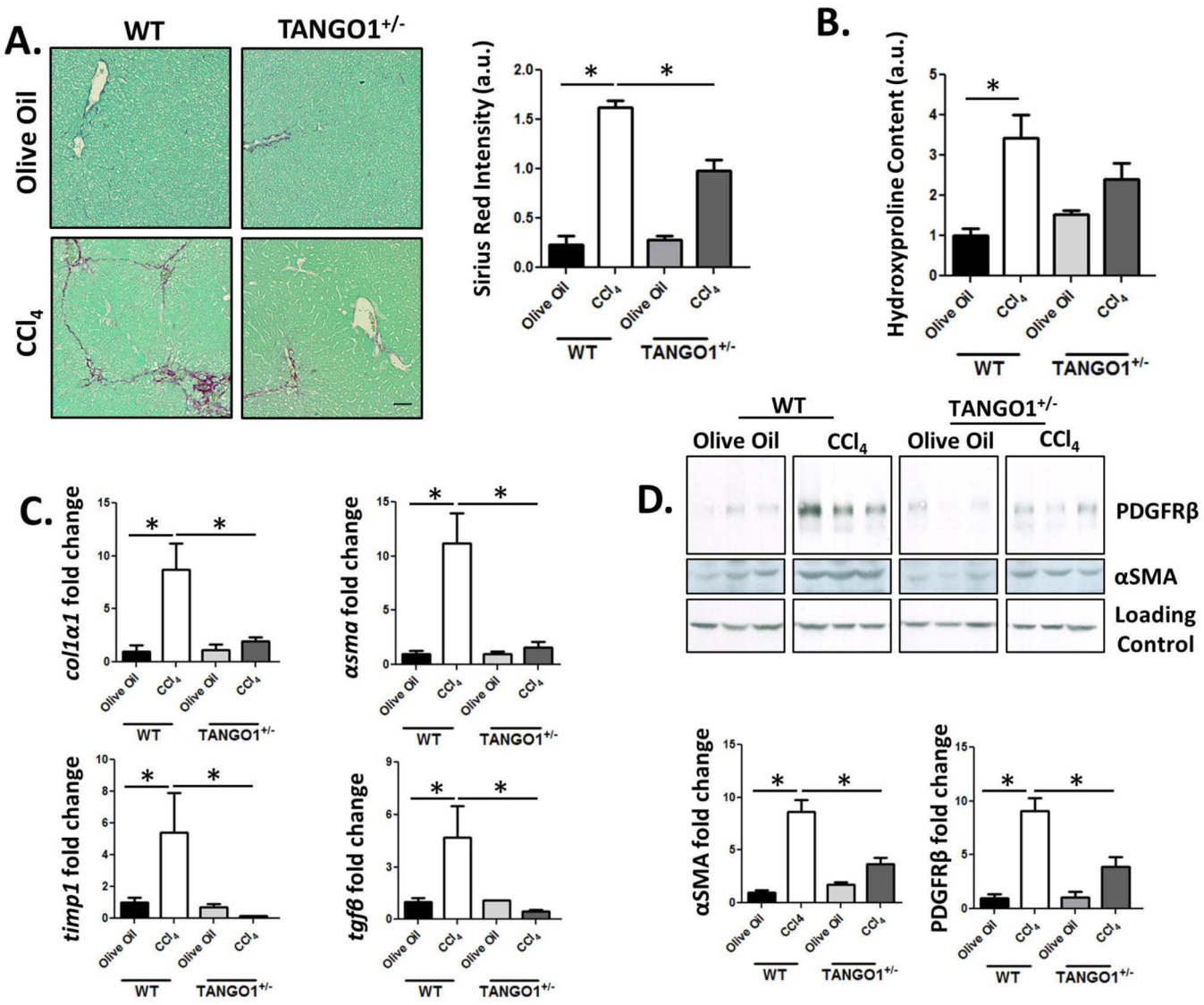

Figure 7. TANGO1$^{+/-}$ mice display decreased fibrosis

A and B. Collagen I content is reduced in livers of TANGO1$^{+/-}$ mice treated with CCL_4 compared to matched WT controls as assayed by Sirius Red staining (A, quantification in adjacent panel, scale bar=100um) and hydroxyproline content (B), (*=p<0.01). C. mRNA harvested from whole liver was reverse transcribed and qPCR was performed to analyze *αSMA, col1α1, tgfβ*, and *timp1* expression (*=p<0.05). D. Whole liver was homogenized and protein expression was analyzed using SDS-PAGE followed by immunoblotting for αSMA and PDGFRβ. Quantification is below. *=p<0.05

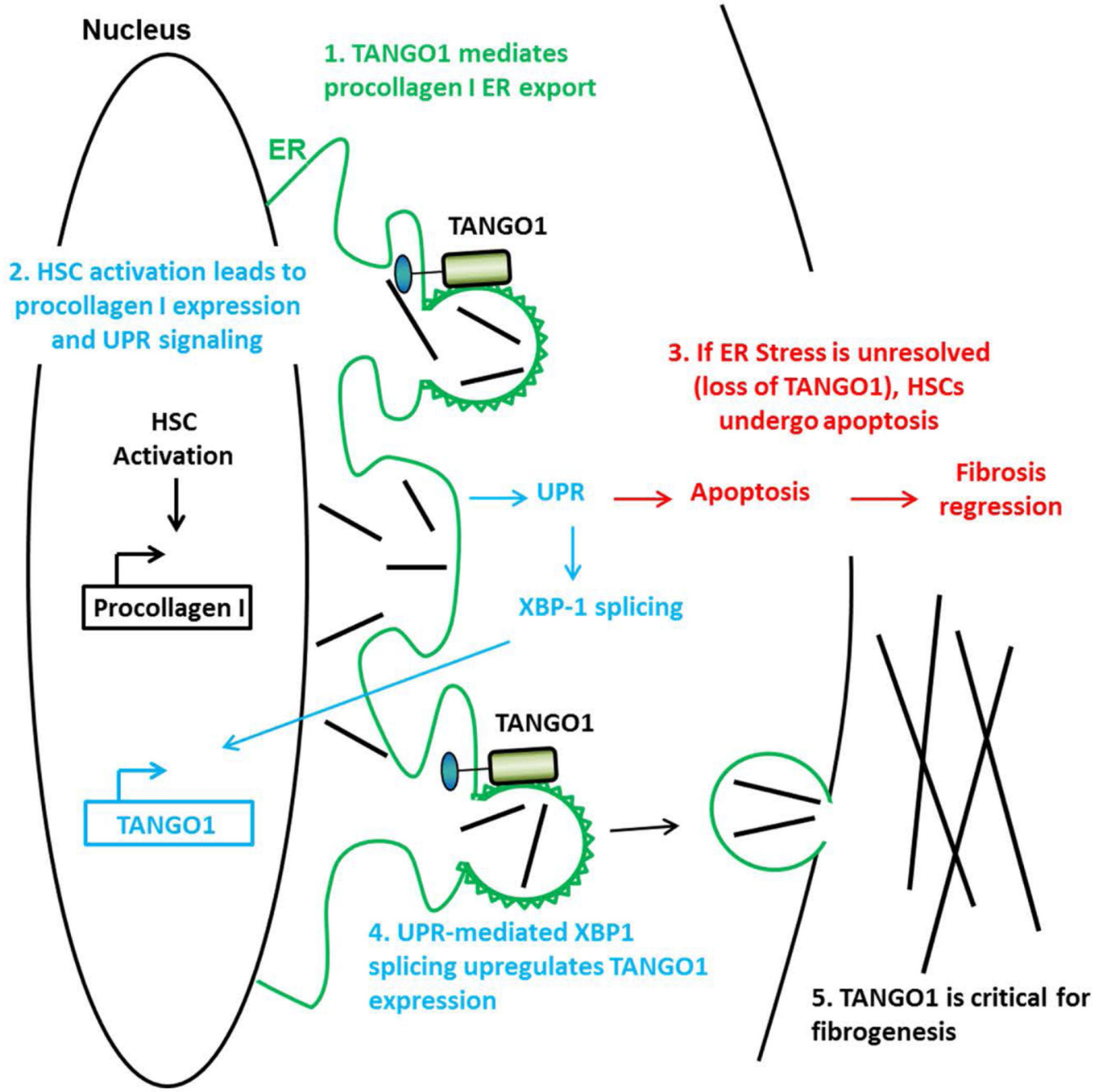

Figure 8. TANGO1 is critical for collagen I secretion and fibrogenesis and is regulated by the UPR

Our data indicates a model wherein TANGO1 is critical for the ER export of procollagen I and its subsequent secretion [1]. Upon HSC activation, procollagen I transcription is increased, leading to ER stress and activation of the UPR [2]. If TANGO1 is lost, ER stress is unable to be resolved and HSC apoptosis occurs [3]. UPR signaling leads to phosphorylation of IRE1α, which then facilitates splicing of the transcription factor XBP1

[4]. XBP1 then translocates to the nucleus and upregulates expression of TANGO1. TANGO1 then facilitates ER export of procollagen I and fibrogenesis [5].